FGFR1 function at the earliest stages of mouse limb development plays an indispensable role in subsequent autopod morphogenesis

Cuiling Li[1], Xiaoling Xu[1], Danielle K. Nelson[2], Trevor Williams[2], Michael R. Kuehn[3] and Chu-Xia Deng[1,*]

[1]Genetics of Development and Disease Branch, NIDDK, NIH, 10/9N105, 10 Center Drive, Bethesda, MD 20892, USA
[2]Department of Craniofacial Biology and Cellular and Developmental Biology, University of Colorado Health Sciences Center, 4200 East Ninth Avenue, Denver, CO 80262, USA
[3]Laboratory of Protein Dynamics and Signaling, Center for Cancer Research, National Cancer Institute, NCI-Frederick, Frederick, MD 21702, USA
*Author for correspondence (e-mail: chuxiad@bdg10.niddk.nih.gov)

Accepted 26 August 2005

Development 132, 4755-4764
Published by The Company of Biologists 2005
doi:10.1242/dev.02065

Summary

Fibroblast growth factors (FGFs) and their receptors have been implicated in limb development. However, because of early post-implantation lethality associated with fibroblast growth factor receptor 1 (FGFR1) deficiency, the role of this receptor in limb development remains elusive. To overcome embryonic lethality, we have performed a conditional knockout of *Fgfr1* using the Cre-LoxP approach. We show that Cre-mediated deletion of *Fgfr1* in limb mesenchyme, beginning at a time point slightly after the first sign of initial budding, primarily affects formation of the first one or two digits. In contrast, deletion of *Fgfr1* at an earlier stage, prior to thickening of limb mesenchyme, results in more severe defects, characterized by malformation of the AER, diminished *Shh* expression and the absence of the majority of the autopod skeletal elements. We show that FGFR1 deficiency does not affect cell proliferation. Instead, it triggers cell death and leads to alterations in expression of a number of genes involved in apoptosis and digit patterning, including increased expression of *Bmp4*, *Dkk1* and *Alx4*, and downregulation of *MKP3*. These data demonstrate that FGF/FGFR1 signals play indispensable roles in the early stages of limb initiation, eliciting a profound effect on the later stages of limb development, including cell survival, autopod formation and digit patterning.

Key words: Apoptosis, BMP4, MKP3, DKK1, ALX4

Introduction

The vertebrate limb bud protrudes from the lateral body wall as a consequence of continued proliferation of mesenchymal cells at the appropriate axial levels at a time of reduced proliferation in the rest of the flank (Summerbell and Wolpert, 1973). The outgrowth and patterning of the developing limbs are dependent on three functionally distinct anatomic structures of the limb bud – the apical ectodermal ridge (AER), the zone of polarizing activity (ZPA) and the progress zone (PZ). They work coordinately to establish, over time, the proximal-distal (PD), and anterior-posterior (AP) axes of the limb (reviewed by Coumoul and Deng, 2003; Mariani and Martin, 2003; Martin, 1998; Tabin, 1995; Tickle and Munsterberg, 2001; Xu et al., 1999).

The AER is a specialized region of thickened ectoderm (epithelium) covering the tip of the limb bud. It is essential for the sustained outgrowth of the limb along the PD axis, and the patterning of the limb through its interaction with the underlying mesenchyme. The ZPA is a region of mesenchyme at the posterior margin of the limb bud, where sonic hedgehog (SHH) provides the spatial cues for the growth of the limb bud along the AP axis. The PZ is composed of undifferentiated mesenchymal cells lying beneath the AER. According to the PZ model, the components of the limb (the autopod, zeugopod and stylopod) are determined by the length of time that progenitor cells spend in the PZ (Summerbell et al., 1973). It has been shown that fibroblast growth factors (FGFs) and FGF receptors (FGFRs) are expressed in the limb bud and play critical roles in the initiation, outgrowth and patterning of the limb (reviewed by Coumoul and Deng, 2003; Mariani and Martin, 2003; Martin, 1998; Tabin, 1995; Tickle and Munsterberg, 2001; Xu et al., 1999).

FGF4, 8, 9 and 17 are expressed in the AER, while FGF10 is expressed in mesenchymal cells underlying the AER (Crossley and Martin, 1995; Martin, 1998; Savage et al., 1993; Tickle and Munsterberg, 2001). It has been shown that placing beads soaked in a particular FGF (FGF2, 4, 8 or 10) on the flank of embryos induces the formation of a limb, while limb truncation, caused by removal of the AER, can be overcome by implanting beads soaked with FGF2 or FGF4 into the limb mesenchyme (Fallon et al., 1994; Niswander and Martin, 1993). In addition, targeted deletion of *Fgf4* and *Fgf8* in the AER generates limbless embryos at birth (Boulet et al., 2004; Sun et al., 2002). Notably, *Fgf4* and *Fgf8* double mutant limb buds are abnormally small although they initiate normally. Increased apoptosis was found in limb mesenchyme, suggesting that AER FGF serves as a survival factor regulating the number of precursor cells of the nascent limb.

FGF receptors contain, in their full-length form, a hydrophobic leader sequence, three immunoglobulin-like (IgI,

II, and III) domains, an acidic box, a transmembrane domain, and a divided tyrosine kinase domain. Many isoforms can be generated through alternative splicing and polyadenylation. For example, alternative splicing at the 5′ region of the *Fgfr1* locus generates FGFR1α (containing three Ig loops), FGFR1β (containing two Ig loops) and FGFR1γ (identical to FGFR1β except it lacks the signal sequence for membrane translocation). Similarly, variable splicing of exons encoding the IgIII domain yield b and c isoforms of FGFR1, 2 and 3 (Hou et al., 1991; Werner et al., 1992). FGFR2b and FGFR2c isoforms are differentially expressed in ectoderm and mesenchyme of the limb bud and mediate signals of mesenchyme-based FGFs (i.e. FGF10) and ectodermal-based FGFs (i.e. FGF8), respectively. Thus, targeted disruption of *Fgfr2* blocks FGF signaling from both mesenchyme and ectoderm, leading to mutant embryos without limb buds (Arman et al., 1999; Li et al., 2001; Xu et al., 1998). Mutant embryos carrying hypomorphic mutations of FGFR2 exhibit abnormal development of limbs with varying severity (Revest et al., 2001).

Unlike *Fgfr2*, *Fgfr1* is primarily expressed in the mesenchyme of developing limb buds. Several lines of evidence indicate that FGFR1 also has important roles in limb development. Human patients carrying a missense mutation (Pro252Arg) that activates FGFR1 display broad toes and split thumbs (Muenke et al., 1994). Transgenic mice bearing four copies of Pro250Arg genomic DNA exhibited an extra digit 1 (Hajihosseini et al., 2004). Conversely, reduced FGFR1 signaling affected development and patterning of the distal limb structures (Partanen et al., 1998). We have previously shown that mutant embryos carrying a targeted deletion of the FGFR1α isoform exhibited distal truncation before they died at E12.5 (Xu et al., 1999). As the tip of the limb is the position of the PZ, it is conceivable that FGFR1-mediated signals play an important role in PZ formation and/or maintenance.

The potential impact of a complete loss of FGFR1 function on limb development has not been assessed because of the early post-implantation lethality of the FGFR1-null mutant (Deng et al., 1994; Yamaguchi et al., 1994). Therefore, we have created an *Fgfr1* conditional allele by flanking exons eight to 14 with loxP sites. In this study, we have used two different Cre lines to ablate FGFR1 at two slightly different time points during the early stages of limb development. This has revealed a narrow window in which FGFR1 signaling is essential for cell survival and autopod morphogenesis occurring at later stages.

Materials and methods

Mice and genotyping analysis

Wild-type and *Fgfr1* conditional mutant mice (Xu et al., 2002) were genotyped by PCR using a pair of primers flanking the third loxP site: forward primer (5′ CTG GTA TCC TGT GCC TAT C 3′) and reverse primer (5′ CAA TCT GAT CCC AAGACC AC 3′). The wild-type allele PCR product is about 400 bp and the conditional allele is about 460 bp. We used a pair of common Cre primers, Cre-1 (5′ CCT GTT TTG CAC GTT CAC CG 3′) and Cre-3 (5′ ATG CTT CTG TCC GTT TGC CG 3′), to genotype both *Ap-2Cre* (Nelson and Williams, 2004) and *Hoxb6-Cre* mice (Lowe et al., 2000). Animals were handled in accordance with guidelines of the NIDDK Animal Care and Users Committee.

Whole-mount in situ hybridization

Whole-mount in situ hybridization was carried out as described previously (Riddle et al., 1993). Anti-sense RNA probes were synthesized using the DIG RNA Labeling Kit (Roche Diagnostics, Mannheim, Germany) according to the manufacturer's recommendations. Probes for the following genes were used: aristaless 4 (*Alx4*), bone morphogenic protein (*Bmp4*), dickkopf homolog 1 (*Dkk1*), engrailed 2 (*En2*), *Fgf4*, *Fgf8*, *Fgfr1*, homeo box D11, 12 and 13 (*Hoxd11*, *Hoxd12*, *Hoxd13*), dual specificity phosphate 6 (*MKP3/Dusp6*), homeo box, msh-like 1 and 2 (*Msx1*, *Msx2*), sonic hedgehog (*Shh*), SRY-box containing gene 9 (*Sox9*), T-box 2 and 3 (*Tbx2*, *Tbx3*) and wingless-related MMTV integration site 7A (*Wnt7a*).

X-gal staining

Embryos were stained in X-gal overnight at 37°C as described previously (Mansour et al., 1993). Embryos were washed in PBS twice after staining, then fixed in 4% paraformaldehyde for 1 hour, dehydrated through a graded alcohol series, treated with xylene, and embedded in paraffin. Eight μm sections were prepared and counterstained with Harris Hematoxylin according to standard procedures.

Whole-mount skeletal preparation

Animals were sacrificed by asphyxiation in CO_2. After removing the skin, carcasses were eviscerated, fixed in 95% ethanol, stained with Alizarin Red S and Alcian Blue, cleared by KOH treatment, then stored in glycerol as described previously (McLeod, 1980).

Detection of apoptotic and proliferating cells

The TUNEL assay was used to detect apoptotic cells in 6 μm sections of paraffin-embedded tissue using a kit obtained from Chemicon International (Temecula, CA, USA). Cell death was detected by staining with LysoTracker Red DND-99 (Molecular Probes, Eugene, OR, USA) using a procedure described by Zucker et al. (Zucker et al., 1999). For detecting cell proliferation in embryos, pregnant mice were injected intraperitoneally with BrdU at a dose of 250 μg/g, and were sacrificed 2 hours later. Immunohistochemical staining for BrdU was performed using an antibody from Becton-Dickinson (South San Francisco, CA, USA) according to the manufacturer's instructions.

Results

Targeted disruption of *Fgfr1* in the distal mesenchyme of the limb bud using *Ap-2Cre*

To study the role of FGFR1 during limb formation and development, we first crossed mice carrying a *Fgfr1* conditional allele ($Fgfr1^{Co}$) (Xu et al., 2002) with *Ap-2Cre* transgenic mice, which express *Cre* in the progress zone of the mouse limb at embryonic day 10.5 (E10.5) (Nelson and Williams, 2004). $Fgfr1^{Co/+}$;*Ap-2Cre* mice were normal and were further crossed with $Fgfr1^{Co/+}$ mice to generate $Fgfr1^{Co/Co}$*Ap-2Cre* mice.

The mouse forelimb bud initiates at early embryonic day 9 (16-17 pairs of somites). Using the Rosa26-β-gal reporter line (R26R) (Soriano, 1999), the Cre activity was first detected in the distal portion of embryos with 20 pairs of somites (Fig. 1A). As the limb bud continued to grow, the area of β-gal-positive cells gradually extended proximally (Fig. 1B,C) and by E11.5 covered the entire limb bud except for the AER (Fig. 1E,F). Of note, the distribution of β-gal-positive cells was biased toward the anterior-distal portion of the forelimb buds at E10.5 (Fig. 1C). Similarly, Cre activity was also first detected at the tip of the hindlimb bud and the area of β-gal-positive cells gradually extended proximally to the entire limb

bud at E11.5 (Fig. 1E,F). The biased pattern of β-gal-positive cells observed in the forelimb was less obvious in the hindlimb buds (Fig. 1D). Using whole-mount in situ hybridization we detected diminished *Fgfr1* transcripts in both the forelimbs and hindlimbs of *Fgfr1*$^{Co/Co}$*Ap-2Cre* mice (Fig. 1G, and not shown). These observations indicate that *Ap-2Cre* may be suitable for studying gene function at stages immediately past limb bud initiation.

Abnormal anterior digit formation in the *Fgfr1*$^{Co/Co}$*;Ap-2Cre* mice

Limb buds of *Fgfr1*$^{Co/Co}$*;Ap-2Cre* mice initiated normally, consistent with our observation that the Cre activity was not detected at the earliest stages of limb initiation. However, abnormal development was detected in both forelimb and hindlimb buds of E11.5 *Fgfr1*$^{Co/Co}$*;Ap-2Cre* embryos, which was characterized by an anterior-distal truncation (Fig. 2A, and not shown). This phenotype was also found in forelimb buds of E10.5 mutant embryos with less severity (not shown). At E12.5, when mesenchyme cells condense to form digits in control mice, the pattern of digit formation was abnormal in the mutant limbs (Fig. 2B). This finding was highlighted by an altered pattern of *Sox9* expression, a gene expressed in digit primordia, which demonstrated that the anterior portion of both the forelimbs and hindlimbs of the *Fgfr1*$^{Co/Co}$*;AP-2Cre* mice had a reduced number of digits and abnormal digit formation (Fig. 2B, and not shown). Abnormal development of anterior digits was confirmed by in situ hybridization with *Hoxd12*, which labels digits two to five, but not the first digit in E12.5-14.5 wild-type limbs (Fig. 2C,D, and not shown). We found that all (n>20) the mutant forelimbs (Fig. 2C) and hindlimbs (Fig. 2D) contained only three (Fig. 2C,D Mt-1) or four (Fig. 2C,D, Mt-2) digits, and they were all *Hoxd12* positive, indicating that the first digit was missing.

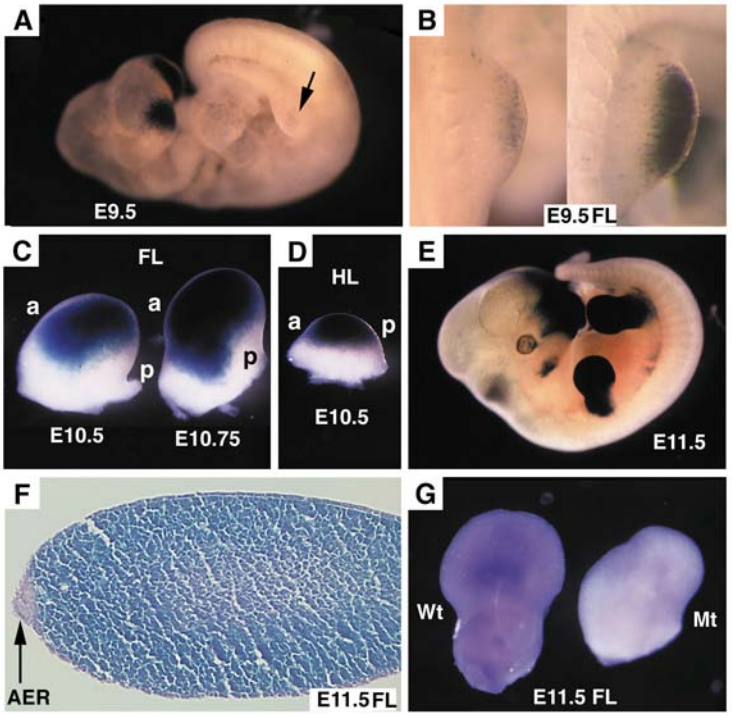

Fig. 1. Activity of *Ap-2Cre* revealed using Rosa-26 reporter mice. Ages of embryos are as indicated. (A) Whole embryo at the 20-somite stage. (B) Forelimbs at the 20 (left) and 28 (right)-somite stage. The embryo in B was slightly bigger than embryo in A. (C) Forelimbs of embryos at the 32 (left) and 36 (right)-somite stage. (D) Hindlimb of an E10.5 embryo (32 somites). (F) Section of E11.5 forelimbs. (G) Whole-mount in situ hybridization of E11.5 forelimbs using a probe for *Fgfr1*. Genotypes of the embryos were: mutant (Mt) *Fgfr1*$^{Co/Co}$*;Ap-2Cre* and controls (Wt) *Fgfr1*$^{Co/Co}$. FL, forelimb; HL, hindlimb; AER, apical ectodermal ridge; a, anterior; p, posterior.

Limb development was analyzed further by Alizarin Red and Alcian Blue staining. Analysis of new born (Fig. 2E,F,G) and postnatal (P) 10 day (Fig. 2H,I) mice revealed that all mutant limbs only had three or four digits with partial fusion at multiple positions (arrows in Fig. 2F,G,H). The first digit of mutant forelimbs was either missing (not shown) or, more frequently, fused with the second digit so that only one abnormal digit was formed (Fig. 2E,F). In contrast, fusion of the first two digits was not observed in mutant hindlimbs. Instead, the limbs only had four digits (Fig. 2G), or three digits (Fig. 2I). No obvious abnormalities in stylopod and zeugopod cartilage in mutant limbs were observed.

To study the underlying mechanisms leading to abnormal digit formation and patterning, we analyzed a number of genes that are expressed along the PD and/or the AP axes. Whole-mount in situ hybridization with *Fgf8* revealed that mutant limb buds have an enlargement of the AER, primarily of the anterior half (Fig. 3A,B). The expression of *Fgf8* in the posterior portion of the mutant AER was either unchanged or only slightly stronger (Fig. 3A,C). FGF signaling in the AER plays an essential role in maintaining expression of SHH in the ZPA (Laufer et al., 1994; Niswander et al., 1994). Consistent with the observation that there was no significant alteration of *Fgf8* and *Fgf4* (not shown) in the posterior half of the AER, expression of *Shh* was not altered (Fig. 3C), indicating that this function of AER FGF signaling is not disrupted. Moreover, examination of a number of other genes, including *Msx1* and *Msx2* (Fig. 3D,E), *Hoxd11-13* (Fig. 3F, and not shown), and *Bmp4* (Fig. 3G), did not reveal obvious changes in their expression in the posterior portions of the E11.5 (Fig. 3D-G) and E12.5 (Fig. 3H, and not shown) limbs. Thus, deletion of *Fgfr1* using *Ap-2Cre* does not have an obvious effect on the posterior-distal portion of the limb at its early stages of development, which may account for the relatively normal morphology of posterior portions of the limbs at later stages of development (Fig. 2E-I).

In contrast, all mutant limbs displayed truncation of the anterior-distal mesenchyme located underneath the enlarged AER (Fig. 3A,B). Whole-mount in situ hybridization using probes for *Msx1* (Fig. 3D), *Msx2* (Fig. 3E) and *Hoxd13* (Fig. 3F) revealed that the anterior-distal portion of the expression domain of these genes was truncated in both the forelimb and the hindlimb of the *Fgfr1*$^{Co/Co}$*;AP-2Cre* mice. BMP signals play important roles in determining digit identity, and haploinsufficiency for BMP4 causes polydactyly in anterior digits (Dunn et al., 1997; Guha et al., 2002; Katagiri et al., 1998). Examination of *Bmp4*, which is expressed in both the AER and the underlying mesenchyme, revealed significantly

increased expression in the AER (Fig. 3G) similar to *Fgf8* (Fig. 3A), while expression in the anterior distal mesenchyme underneath the AER was markedly reduced (Fig. 3G). Because BMP signaling induces apoptosis in developing limbs (Guha et al., 2002), the observed truncations may result from increased expression of AER-BMP inducing an abnormally high level of apoptosis in the mutant limbs (see Discussion).

In summary, our analysis of Ap2-Cre deletion of *Fgfr1* reveals specific loss in the distal mesenchyme resulting in abnormal development of the anterior digits. There is only a mild impact on the formation of posterior digits, and no or rare effects on proximal skeletal elements. These observations suggest that FGF/FGFR1 signaling plays important roles in anterior digit formation and is less critical for the formation of the posterior digits. However, recent data suggests that the precursors for some skeletal elements of the PD axis might be predetermined at very early stages of limb bud development (Dudley et al., 2002; Sun et al., 2002). Thus, although deletion of *Fgfr1* eventually spreads to the entire limb prior to any detectable morphological signs of mesenchyme differentiation, *AP-2Cre*-mediated deletion of *Fgfr1* may simply be too late to affect the development of posterior digits and the proximal portion of the limb.

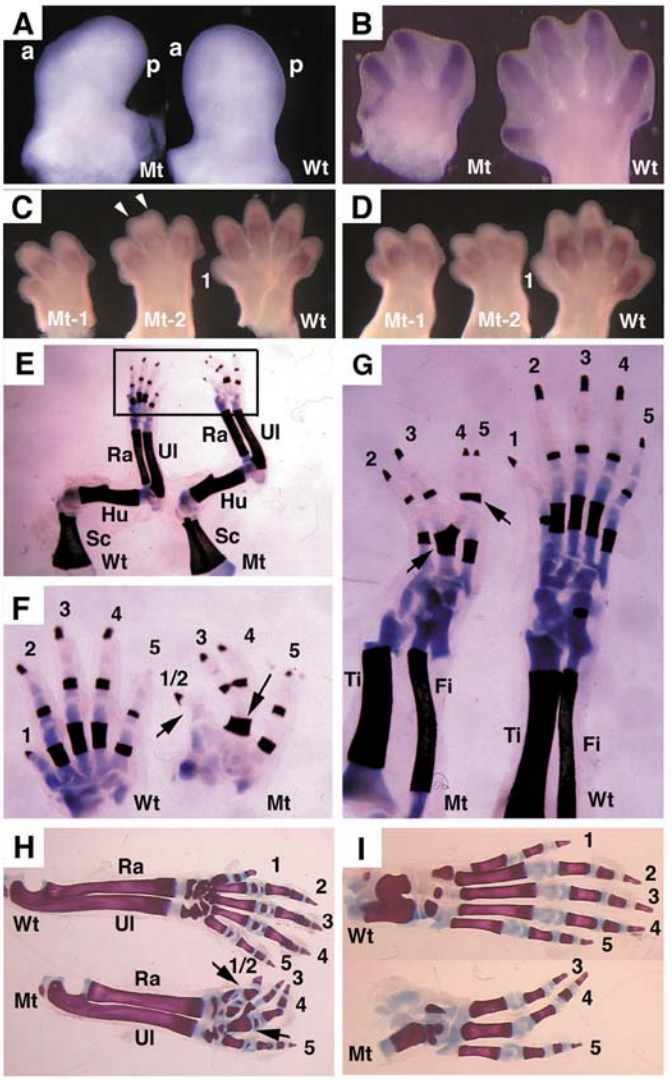

Fig. 2. Abnormal digit formation and limb development in *Fgfr1*$^{Co/Co}$*;Ap-2Cre* mice. (A) Forelimb of E11.5 *Fgfr1*$^{Co/Co}$*;Ap-2Cre* (Mt) and *Fgfr1*$^{Co/Co}$control (Wt) mice. (B) Whole-mount in situ hybridization for *Sox9* in E12 forelimbs. (C,D) *Hoxd12* stained E13.5 forelimbs (C) and hindlimbs (D). The *Hoxd12*-negative digit is the first digit (1). Arrowheads in C indicate fused digits. (E-I) Alizarin Red and Alcian Blue stained newborn forelimbs (E-G), and P10 hindlimbs (H,I). The arrows in F-H indicate fused digits. The boxed area in E is enlarged in F. Ra, radius; Ul, ulna; In, intermedium; Fib, fibulare; Ti, tibia; Fi, fibula; Sc, scapula; Hu, humerus.

Targeted deletion of *Fgfr1* using *Hoxb6-Cre*

To determine how the timing of *Fgfr1* elimination from the limb bud might impact morphogenesis, we deleted *Fgfr1* using *Hoxb6-Cre*, which is expressed throughout the lateral plate mesoderm of E8.5 embryos (6-12 pairs of somites) (Lowe et al., 2000) (Fig. 4A). At E9.5, Cre activity is found in the initial thickening of the mesoderm of the hindlimb bud (25 somites, Fig. 4B) and then in the entire limb at later stages (Fig. 4G). In the forelimb, although Cre activity is detected at the time of limb initiation, it starts posteriorly and then gradually extends towards the anterior portion of the limb (20 somites, Fig. 4C and not shown). At late E9.5, β-gal-positive cells populate

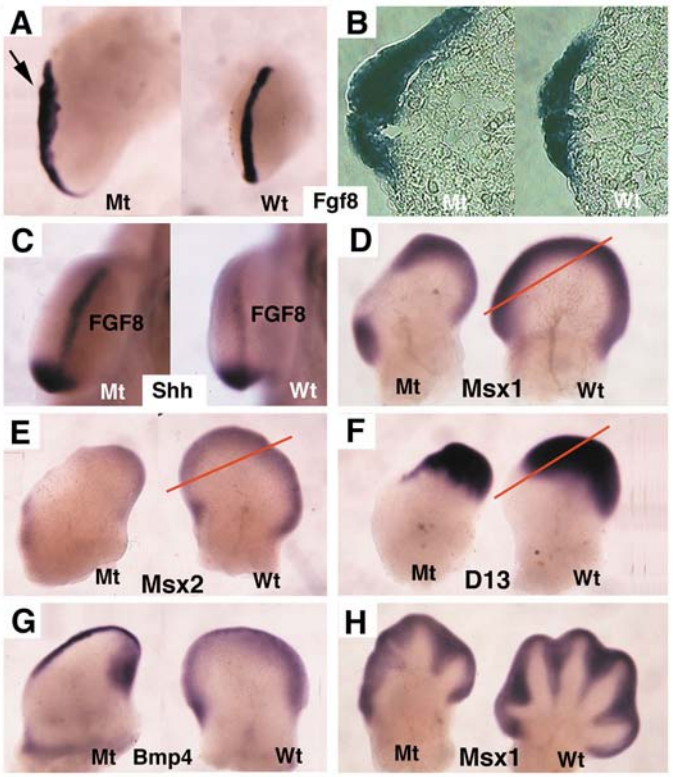

Fig. 3. Anterior-distal abnormalities in *Fgfr1*$^{Co/Co}$*;Ap-2Cre* limbs. Whole-mount in situ hybridization probes were as indicated. Ages of limb buds were E11.5 (A,B,D-G), E10.5 (C) and E12.5 (H). Arrow in A indicates the enlarged anterior portion of the AER. Frozen sections of limb buds in A are shown in B. Note, samples shown in C were hybridized with probes for *Fgf8* and *Shh* simultaneously. The red lines in D-F mark the corresponding position of truncation in mutant limbs. Wt, wild type; Mt, mutant.

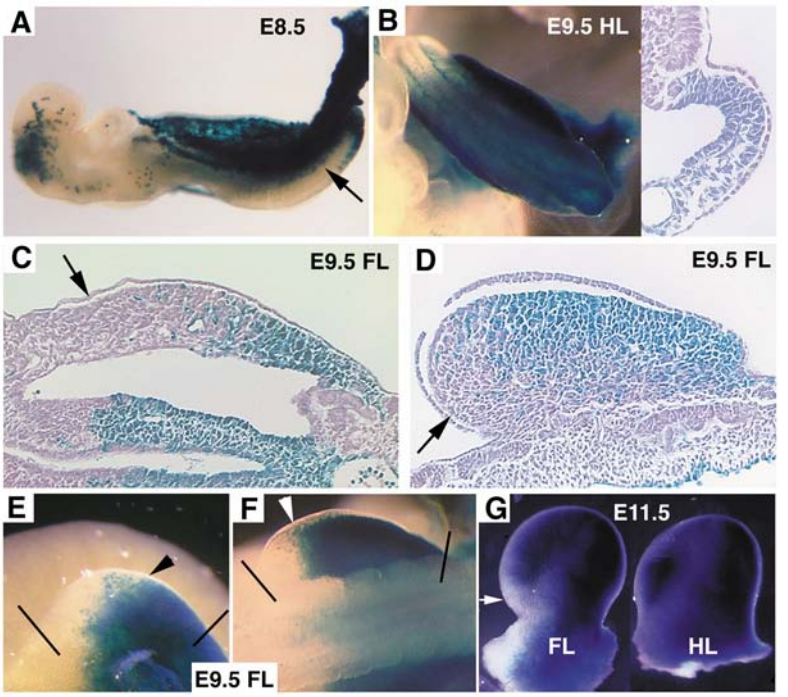

Fig. 4. Activity of *Hoxb6-Cre* revealed by analysis of Rosa-26 reporter mice. Ages of embryos are as indicated; the number of pairs of somites are: 8 (A), 25 (B,D,F), 20 (C) and 22 (E) pairs of somites. The arrow in A indicates the presumptive hindlimb territory. Arrows in C,D,G indicate anterior areas lacking Cre activity. In E and F the extent of the forelimbs is marked with lines. The arrowheads indicate a boundary between solid blue and diffuse β-gal staining, indicating that Cre activity gradually extends anteriorly. FL, forelimb; HL, hindlimb.

significant portions of the limb (Fig. 4D,E,F) and by E11.5 nearly the entire limb bud is positive except for a small area in the anterior-proximal region (arrow, Fig. 4G). These data suggest that *Hoxb6-Cre* is an ideal tool to study gene function during the early stages of hindlimb development, but not for the early stages of forelimb development, except if there is a specific need to study genes in the posterior domains of the forelimb.

Severe abnormalities in autopod formation in hindlimbs of *Fgfr1$^{Co/Co}$;Hoxb6-Cre* mice

Despite the expression of *Hoxb6-Cre* in the entire hindlimb at its earliest stages of initiation, *Fgfr1$^{Co/Co}$;Hoxb6-Cre* mice displayed no obvious abnormalities in hindlimbs prior to E10.5 (not shown). However, at E10.75, the hindlimb buds of *Fgfr1$^{Co/Co}$;Hoxb6-Cre* mice displayed a reduced height along the PD axis and an extended length along the AP axis (Fig. 5A). The AER of mutant embryos was thicker and shorter than that of control mice as revealed by expression of *Fgf8* (Fig. 5A) and *Fgf4* (not shown). At E11.5, the AER of mutant hindlimbs was significantly shorter than that of controls and distorted (Fig. 5B). Concurrent with these abnormalities, the expression of *Shh* in the ZPA was significantly weaker (Fig. 5C). Because FGF4 and FGF8 double null hindlimbs do not express *Shh* (Boulet et al., 2004; Sun et al., 2002), we believe that FGFR1 deficiency impairs, but does not completely block, FGF signaling in the posterior portion of the AER, thus maintaining limb outgrowth along the PD axis.

It has been shown that SHH negatively regulates expression of the aristaless-like transcription factor 4 (*Alx4*) (Takahashi et al., 1998). Along with markedly reduced *Shh* expression, we detected a significant expansion of *Alx4* expression in the anterior of mutant limb buds (Fig. 5D). This expansion also correlates well with the hypoplasia of the anterior portion of the mutant limbs, which is consistent with a finding that targeted disruption of *Alx4* resulted in preaxial polydactyly of the anterior digits (Qu et al., 1997). To determine the effect of FGFR1 deficiency on the development of posterior portion of the limb, we examined expression of *Tbx2* and *Tbx3*. Both are expressed in the interdigit region between the fourth and fifth digits and in the posterior margin of the limb, and play roles in patterning the most posterior two digits in the mouse (Davenport et al., 2003) and chicken (Suzuki et al., 2004). Our data revealed that expression of both *Tbx2* and *Tbx3* was maintained in the posterior region of the mutant limbs (Fig. 5E,F), suggesting that this part was less affected. All the mutant limbs examined at E11.5-E12.5 also exhibited increased length along the dorsal-ventral (DV) axis (Fig. 5B,G). However, our in situ hybridization using probes for *Wnt7a* and *En2*, which play a key role in the establishment of the DV axis, did not reveal any obvious changes of their expression patterns and intensities (not shown), suggesting that

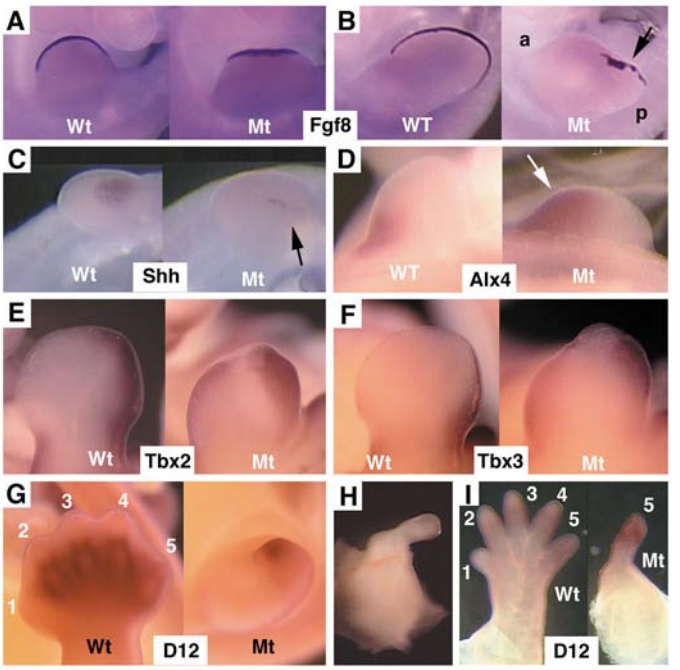

Fig. 5. Malformation of hindlimbs of *Fgfr1$^{Co/Co}$;Hoxb6-Cre* mice. Images of E10.5 (A,C,D), E11.5 (B), E12.25 (E,F), E12.5 (G) and E14.5 (H,I) limbs. Probes used for whole-mount in situ hybridization are as indicated. Anterior is to the left and posterior to the right in all the panels. Arrows indicate the abnormal AER (B), the significantly reduced *Shh* expression (C), and the expanded *Alx4* expression domain (D). Wt, wild type; Mt, mutant.

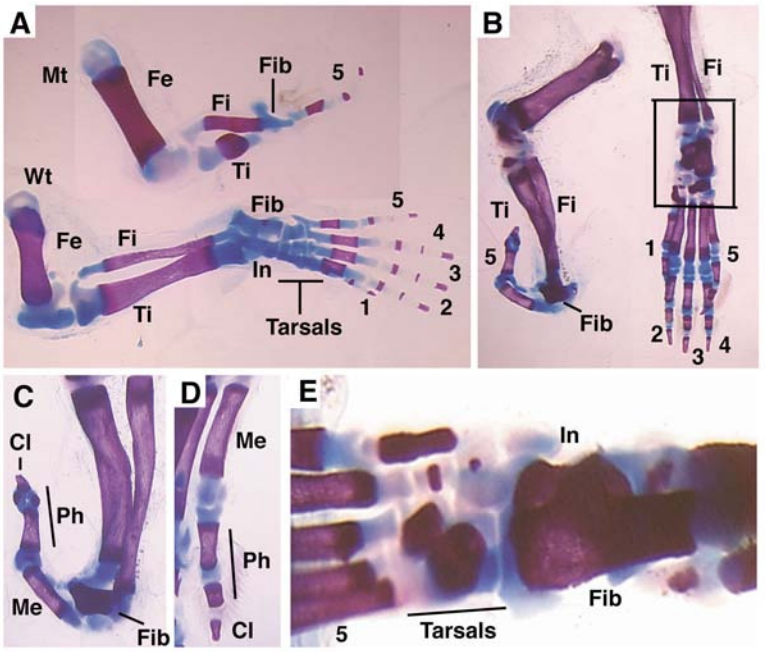

Fig. 6. Abnormal autopod formation and patterning in *Fgfr1*$^{Co/Co}$*;Hoxb6-Cre* mice. (A,B) Alizarin Red and Alcian Blue stained P1 (A) and P10 (B) hindlimbs. (C,D) Higher magnification of the fifth digit of a mutant (C), and a wild type (D). The boxed area in B is enlarged in E. Cl, claw; Fib, fibulare; In, intermedium; Ph, phalanges; Wt, wild type; Mt, mutant.

this phenotype may be secondary to the reduced height of the PD axis.

At E12.5, primordia of all five digits are observed in the wild-type limb, with the first digit negative for the expression of *Hoxd12*, and the remaining digits positively labeled (Fig. 5G). However, in the mutant limb, only one *Hoxd12*-positive protrusion was visible (Fig. 5G). This protrusion continued to develop into a distinct digit by E14.5 (Fig. 5H). We postulate that this *Hoxd12*-expressing protrusion is not digit one, because *Hoxd12* is normally expressed at a much lower level in the first digit than it is in digits two to five of E14.5 wild-type limbs (Fig. 5I). Given the hypoplasia observed in the anterior portion of the mutant limbs at earlier stages (Fig. 5E-G), we suspected that it might be the fifth digit. Analysis of mutant limbs at later stages of development revealed that this digit was connected to the fibulare (calcaneum) (Fig. 6A,B), supporting the hypothesis that it is the fifth digit. However, the absolute identity of this digit is difficult to determine because of the lack of specific molecular markers for the individual digits. Of further note, mutant hindlimbs exhibited severe defects in ankle formation, missing all the tarsals and only having a fibulare (Fig. 6A-D). Some mutant hindlimbs also exhibited impaired ossification of the fibula (not shown) and/or the tibia (Fig. 6A). Taken together, our data indicate that deletion of *Fgfr1* using *Hoxb6-Cre* yields much more severe hindlimb abnormalities than obtained when using *Ap-2Cre,* presumably because *Hoxb6-Cre* is expressed at earlier stages of limb bud initiation.

The finding that disruption of FGFR1 by *Hoxb6-Cre* does not block formation of the most posterior digit could be due to a number of factors, such as incomplete deletion of FGFR1 by Cre and/or functional redundancy with other member(s) of the FGF receptor family. For the latter, a good candidate is FGFR2 because it is expressed in both the AER and underlying mesenchyme of the limb at these stages of development (Orr-Urtreger et al., 1993; Xu et al., 1998).

Phenotypes of forelimbs of *Fgfr1*$^{Co/Co}$*;Hoxb6-Cre* mice

Our analysis of mutant limbs thus far indicates that severe phenotypes are associated with FGFR1 deletion at the earliest stages of limb development, while deletion at slightly later stages immediately after initial budding has a much milder effect. Because *Hoxb6-Cre* is first expressed in the posterior portion of the forelimb prior to its budding and the expression domain gradually extends to the anterior at later stages, we predict that abnormalities may only occur in the most posterior part of the forelimb, while the anterior portions, which express Cre at slightly late stages, should only have minor or even no

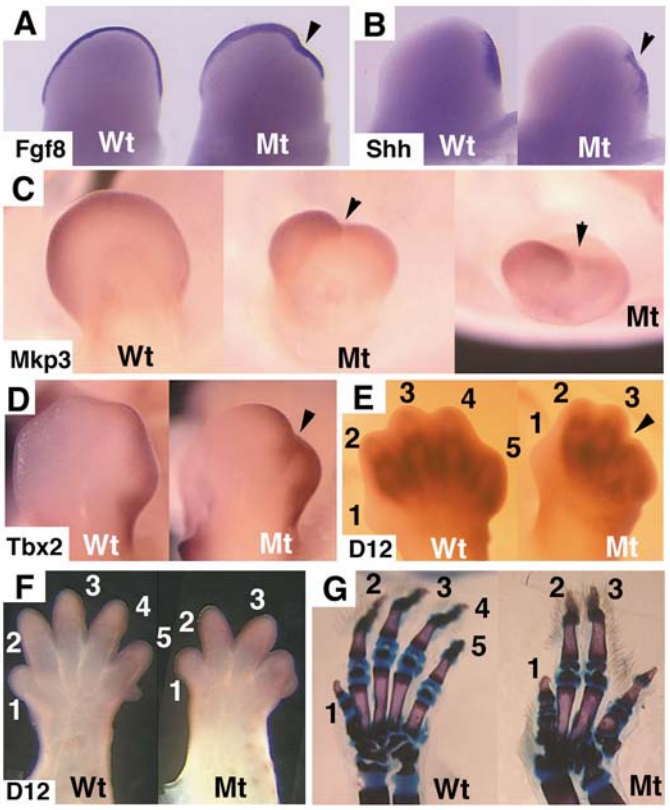

Fig. 7. Phenotypes of forelimbs of *Fgfr1*$^{Co/Co}$*;Hoxb6-Cre* mice. Whole-mount in situ hybridization using probes as indicated. Ages of limb buds were E11.5 (A,B), E12.25 (C), E12.5 (D,E), E14.5 (F) and P21 (G). Arrowheads in A-E indicate the border between the relatively normal anterior and the abnormal posterior portions of the limbs. The mutant limb bud shown in C is placed at two different angles to show a reduced height for the PD axis (middle) and an increased length of the DV axis (right). Wt, wild type; Mt, mutant.

visible defects. Indeed, analysis of forelimbs of *Fgfr1*$^{Co/Co}$*;Hoxb6-Cre* mice revealed a reduced height for the PD axis (Fig. 7A-D) and an increased length along the DV axis (Fig. 7C) only in the posterior region. These phenotypes started at E10.75 and were obvious by E11.5 with some variations. Whole-mount in situ hybridization using *Hoxd12* revealed a normal appearance of the first two or three digits while the development of the posterior digits was abnormal (Fig. 7E, and not shown). These data indicate that deletion of FGFR1 does not affect anterior digit formation despite Cre activity having spread through the entire distal portions of the limb prior to digit formation (Fig. 4G). Of note, the areas showing abnormalities in mutant embryos examined from E9.5-E12.5 (n>30) were always smaller than the β-gal positive areas in reporter mice. This indicates the abnormalities only occur in the region where *Hoxb6-Cre* is first expressed, i.e. prior to or during the initial budding, and not in the more anterior regions, to where Cre expression spreads by slightly later stages. This is consistent with what was observed in *Fgfr1*$^{Co/Co}$*;AP-2Cre* mice.

Next, we stained the forelimbs of *Fgfr1*$^{Co/Co}$*;Hoxb6-Cre* mice using Alcian Blue and Alizarin Red staining. This revealed that most mutant forelimbs contained only four digits (Fig. 7G), while one mutant limb had only three digits (not shown). Whole-mount in situ hybridization of E12.5 limbs using *Tbx2* and *Tbx3* revealed relatively normal expression in the interdigit region between the fourth and the fifth digits and in the posterior margin of the mutant forelimbs (Fig. 7D and not shown). This suggests that the mutant limb contains the primordium for the fifth digit at this stage of development. Therefore we postulate that, similar to the hindlimb of *Fgfr1*$^{Co/Co}$*;Hoxb6-Cre* mice, the last digit in the forelimb is digit five and it was able to grow. This is perhaps because of the expression of SHH and/or HOXD12 and 13 (Fig. 7B,E,F, and not shown), all of which are known to play an important role in digit formation, patterning and specification (Chen et al., 2004; Chiang et al., 1996; Davis and Capecchi, 1996; Zakany and Duboule, 1996; Zakany et al., 2004).

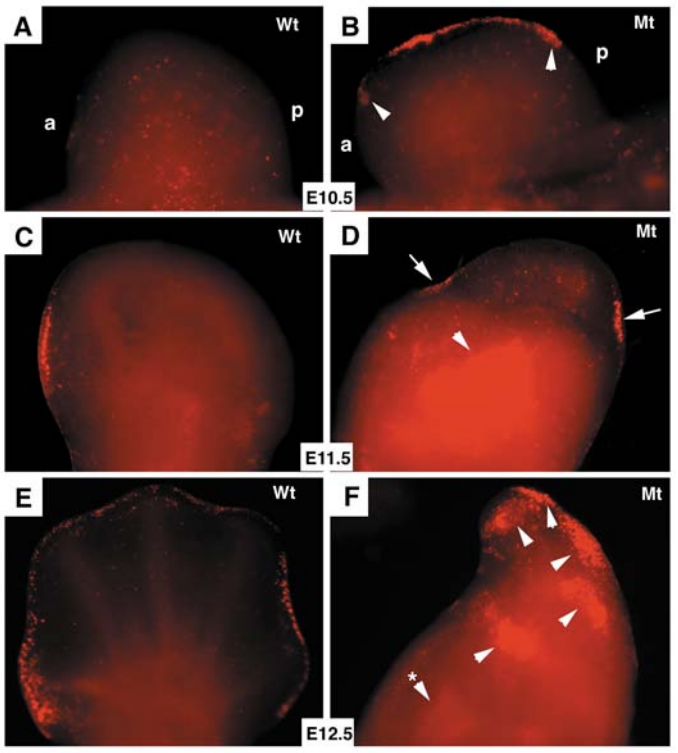

Fig. 8. Increased apoptosis in the hindlimbs of *Fgfr1*$^{Co/Co}$*;Hoxb6-Cre* mice detected by staining with LysoTracker Red. Whole-mount images of E10.5 (A,B), E11.5 (C,D) and E12.5 (E,F) limbs. Arrows and arrowheads in mutant limbs indicate apoptotic cells. The arrowhead marked with an asterisk in F indicates an apoptotic area that is out of focus, but it was confirmed under the microscope. Wt, wild type; Mt, mutant.

Increased apoptosis is associated with the absence of FGFR1

Our analysis reveals that the majority of autopod skeletal elements are missing in the hindlimbs of *Fgfr1*$^{Co/Co}$*;Hoxb6-Cre* mice except for the fibulare and the last digit. To investigate the cause of this defect, we studied apoptosis in E10.5-E12.5 embryos. Whole-mount imaging of E10.5 limbs after stained with a vital lysosomal dye, LysoTracker Red, revealed that apoptotic cells were primarily concentrated within the AER of mutant limbs (Fig. 8B). Small amounts of apoptotic cells were also found in the mensenchyme immediately underneath the AER (arrowheads, Fig. 8B). At E11.5, although apoptotic cells were still present in the AER (arrows, Fig. 8D), they were more concentrated in areas about 200 μm away from the AER (arrowhead, Fig. 8D). At E12.5, areas with apoptotic cells had spread to many places in the mutant limbs, including the AER and mesenchyme (Fig. 8F). In contrast, apoptotic cells started to appear in the anterior AER of control limbs at E11.5 (arrow, Fig. 8C) and extended posteriorly to include the entire AER by E12.5 (Fig. 8E). Increased apoptosis was confirmed using the TUNEL assay on histological sections of hindlimbs (Fig. 9B) and posterior portions of forelimbs (see Fig. S1 in the supplementary material) of *Fgfr1*$^{Co/Co}$*;Hoxb6-Cre* mice, and the anterior portions of both fore- and hindlimbs of *Fgfr1*$^{Co/Co}$*;AP-2Cre* mice (Fig. 9D). These observations indicate that FGFR1-mediated FGF signaling plays an important role in maintaining cell survival. We also studied cell proliferation using BrdU incorporation but failed to find any obvious difference between mutant and wild-type limbs (not shown).

We next investigated possible causes for the increased apoptosis using a candidate approach and found alterations in the expression of three genes that are involved in apoptosis. BMP signals play an important role in inducing apoptosis (Guha et al., 2002), and we have shown above that disruption of *Fgfr1* by *AP-2Cre* results in increased expression of *Bmp4* in the AER (Fig. 3I). We detected a similar pattern of increased expression of *Bmp4* in the AER of *Fgfr1*$^{Co/Co}$*;Hoxb6-Cre* limbs and decreased expression in the underlying mesenchyme (Fig. 9E). We also found significant down regulation of MAPK phosphatase 3 (*MKP3*) in mutant hindlimbs (Fig. 9F). Interestingly, it was recently shown that FGF8 positively regulates *MKP3*, and that suppression of *MKP3* by small interfering RNA (siRNA) induced apoptosis in the mesenchyme (Kawakami et al., 2003). We also examined expression of dickkopf 1 (*Dkk1*), which is a negative modulator of the Wnt pathway and has been implicated in programmed cell death during limb development (Mukhopadhyay et al.,

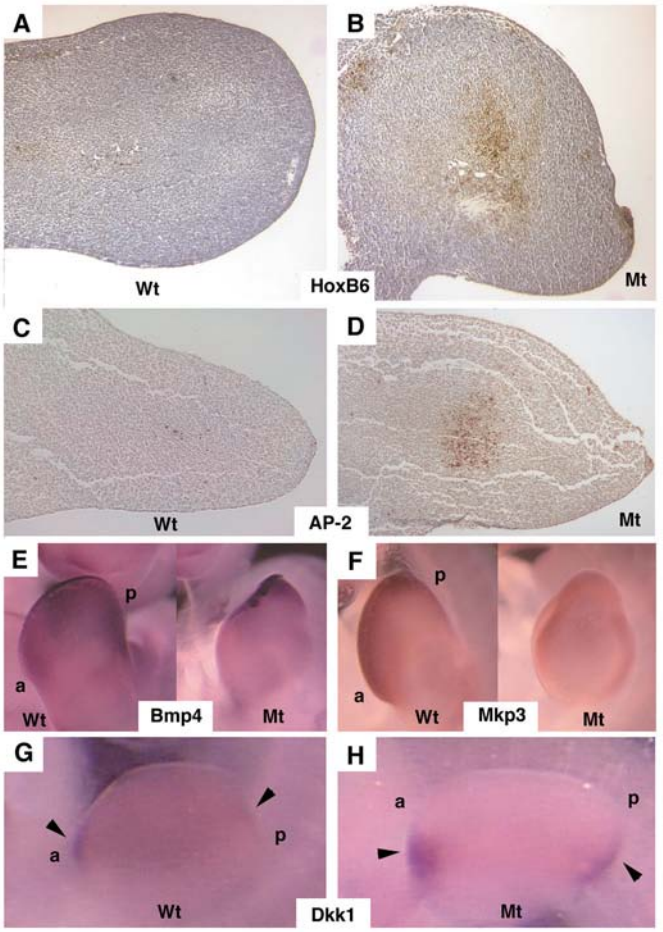

Fig. 9. Increased apoptosis and altered gene expression in FGFR1-deficient limbs. (A-D) TUNEL assay on E11.5 wild type (A,C) and mutant (B,D) limbs. C and D are cross sections of hindlimbs of wild-type (C) and *Fgfr1*$^{Co/Co}$*;AP-2Cre* (D) mice. Note that the mutant limb shown in D is wider because of an increased length of the DV axis, which can only been seen in the cross sections. All other images are hindlimbs of wild type and *Fgfr1*$^{Co/Co}$*;Hoxb6-Cre* mice.
(E-H) Whole-mount in situ hybridization of E10.5 (G,H, arrowheads indicate areas of *Dkk1* expression), and E11.5 (E,F) limbs. Genotypes and probes are as indicated.

2001). *Dkk1* is normally expressed in the anterior proximal margin and the posterior proximal margin of the limb (arrowheads, Fig. 9G). We found that loss of FGFR1 significantly increased expression of *Dkk1* in these areas (Fig. 9H).

Discussion

It has been shown that targeted disruption of AER-FGF signaling results in profound limb defects, ranging from the complete block of limb initiation to defective development of various skeletal elements, depending on the stage at which the FGFs (i.e. FGF4 and FGF8) are knocked out (Boulet et al., 2004; Sun et al., 2002). Two of the four known high affinity FGF receptors, FGFR1 and FGFR2, are expressed during the early stages of limb development, each with a distinct pattern (Orr-Urtreger et al., 1991). It was previously shown that targeted deletion of the IgIII domain of FGFR2 completely blocked limb initiation (Arman et al., 1999; Li et al., 2001; Xu et al., 1998), although the potential roles of this receptor in later stages of limb development are unclear. In the current study, we assessed the roles of FGFR1 signaling in forelimb and hindlimb development by disrupting this gene using two strains of transgenic mice that express Cre recombinase in complementary temporal and spatial patterns during limb bud formation. Our data indicate that disruption of *Fgfr1* at a stage prior to the initial thickening of mesoderm in the hindlimb territory using *Hoxb6-Cre* does not have any obvious impact on limb initiation. Instead, it primarily affects autopod development and patterning. This observation suggests that FGFR1 is dispensable for limb initiation, but has an important role in specifying the proximal-distal development of the limb.

AP-2Cre deletion produced a more consistent mutant forelimb phenotype than *Hoxb6-Cre* and enabled us to compare the consequences of removal of FGFR1 activity at later stages of hindlimb outgrowth. Consistent with the later induction of Cre recombinase, the phenotype of *Fgfr1*$^{Co/Co}$*;AP-2Cre* hindlimbs was milder than that of *Fgfr1*$^{Co/Co}$*;Hoxb6-Cre* limbs, but nevertheless reveals an ongoing requirement for FGF signaling in digit patterning. Moreover, FGFR1 mutant limbs generated by either Cre transgene had several common features, including malformation of the AER and truncation of distal mesenchyme at E10.5-E12.5, followed by abnormal digit development and patterning at later stages. Because neither *AP-2Cre* nor *Hoxb6-Cre* is expressed in the AER, the malformation of the AER must be secondary to abnormalities in the underlying mesenchyme. For example, the increased *Fgf8* expression found in the AER of mutants could be a feedback response to a signaling block in the underlying mesenchyme resulting from loss of receptor. Indeed, we have specifically knocked out *Fgfr1* in the AER using *Msx2-Cre* (Sun et al., 2000), and did not find any obvious abnormalities (data not shown).

We have found hypoplasia of the mesenchyme in FGFR1-deficient limbs and shown that it is associated with an increase in cell death. Increased apoptosis was also observed in limb buds carrying either an *Fgf4*/*Fgf8* double mutation (Boulet et al., 2004; Sun et al., 2002) or a hypomorphic mutation of *Fgfr2* (Revest et al., 2001). Together, these data provide compelling support for the hypothesis that FGF signaling, mediated by FGFR1 and FGFR2, acts as a survival program that regulates the number of precursor cells within the nascent limb mesenchyme (Boulet et al., 2004; Sun et al., 2002). Our data indicate that apoptosis first occurs in the mutant AER and gradually spreads into mesenchyme of the limb. In an effort to identify potential downstream mediators for FGF signaling in cell survival, we have identified four candidate genes, *Bmp4*, *Dkk1*, *MKP3* and *Alx4*, which show significant alterations in their expression pattern and intensity in FGFR1-deficient limbs. Specifically, we detected increased expression of *Bmp4* in the AER, reduced expression of *MKP3* in the distal mesenchyme underneath the AER, an expanded expression domain of *Alx4* in the anterior half of the limb, and increased expression of *Dkk1* in both the anterior proximal and the posterior proximal margins of the limb. Although it remains possible that the altered expression of all or some of these genes is simply a secondary consequence of FGFR1 mutation, previous studies have implicated them in apoptosis and/or digit

patterning (Dunn et al., 1997; Guha et al., 2002; Katagiri et al., 1998; Kawakami et al., 2003; Mukhopadhyay et al., 2001; Qu et al., 1997). It was shown that blocking BMP signaling by over expressing a BMP antagonist, noggin, in limbs of transgenic mice significantly reduced apoptosis, leading to extensive limb soft tissue syndactyly and postaxial polydactyly (Guha et al., 2002). Consistently, polydactyly or ectopic digit formation was observed in the *Bmp4*$^{+/-}$ mice that also carried a heterozygous mutation for *Bmp7*, *Gli3* or *Alx4* (Dunn et al., 1997; Katagiri et al., 1998). We have also found that AER-specific disruption of *Smad4*, which is a common mediator for the TGFβ superfamily, including all BMPs (Heldin et al., 1997; Massague, 1998), reduced apoptosis in interdigit mesenchyme (C.L. and C.-X.D., unpublished data). Despite these observations, however, there is no direct evidence that over expression of *Bmp4* in the AER can induce apoptosis. This issue could be directly tested by expressing this gene in the AER using an AER-specific promoter, such as the *Msx2* promoter, which has been used to target Cre to the AER (Sun et al., 2000). It is interesting that in an independent study using two different transgenic Cre strains, Verheyden et al. also found that the absence of FGFR1 results in extensive apoptosis in limb mesenchyme (Verheyden et al., 2005), providing additional evidence that FGF/FGFR1 signals play an essential role in maintaining cell survival during limb development.

We believe it is a significant finding that the absence of FGFR1 results in down regulation of *MKP3*. MKP3 is a specific and potent regulator of the ERK class of MAP kinases. In the mouse embryo, it was recently demonstrated that regions of FGFR signaling overlap with the strongest domains of ERK activation (Corson et al., 2003), and that FGF8 positively regulates *MKP3* (Kawakami et al., 2003). Moreover, suppression of *MKP3* by small interfering RNA (siRNA) induces apoptosis in the mesenchyme (Kawakami et al., 2003), providing strong evidence that reduced expression of *MKP3* in FGFR1-deficient limbs could be the cause of the increased apoptosis and reduced number of digits. Future studies should be directed to determining how FGF/FGFR1 signaling regulates *MKP3* expression, and the potential relationships among *MKP3*, *Alk4* and *Dkk1* in terms of apoptosis and digit development and patterning.

Another significant finding of this study concerns how the timing of FGFR1 removal alters the ultimate patterning of the limb bud. In contrast to the major hindlimb alterations obtained with *Hoxb6-Cre*, disruption of FGFR1 at a stage immediately after the initial budding of the limb using *AP-2Cre* results in a less severe phenotype that only affects the formation of the first one or two digits. These observations suggest that the action of FGFR1 signaling in specifying the majority of autopod development and patterning occurs at very early stages of limb development. One possibility is that the precursor cells that will develop into the autopod skeletal elements have already been specified by the very early stages of limb development, and once the fate of these cells is determined, FGFR1 signaling becomes less critical to their development. Therefore, the very early disruption of FGFR1 by *Hoxb6-Cre* generates a more profound limb phenotype than the slightly later disruption by *AP-2Cre* even though both transgenes act prior to the overt differentiation of the mesenchyme. Another theoretical explanation for the severe hindlimb abnormalities in *Fgfr1*$^{Co/Co}$*;Hoxb6-Cre* mice is that the removal of FGFR1 in the lateral plate mesoderm causes less mesoderm to be available for recruitment to the limb bud. This hypothesis remains to be tested, although we did find that hindlimbs of E10 and younger *Fgfr1*$^{Co/Co}$*;Hoxb6-Cre* mice were normal in size and contained equivalent number of cells to that of control limbs.

Of note, a new model regarding limb development and patterning along the proximal-distal axis has recently been proposed (Dudley et al., 2002; Sun et al., 2002). According to this model, the components of the limb skeleton (autopod, zeugopod and stylopod) are specified much earlier than assumed by the PZ model (Summerbell et al., 1973), and may be independent of drop-out time. The model further proposes that limb outgrowth is associated with expansion and sequential differentiation of these elements, and that a cell's fate may be determined during the early stages of limb development (Dudley et al., 2002; Sun et al., 2002). While this model is still controversial (Saunders, 2002; Wolpert, 2002), our observations indicate that FGF/FGFR1 signaling may play an indispensable role in the very early stages of limb development, which affects autopod formation and digit patterning at later stages of limb development.

We thank X. Sun for providing probes for *Alx4*, *En2* and *Wnt7a*, S. Keyse for *MKP3*, H. Westphal for *Dkk1,* T. Furusawa for *Sox9* and B.G. Bruneau for *Tbx2* and *Tbx3*. We are grateful to members of the Deng laboratory for helpful discussions and critical reading of the manuscript. This research was supported by the Intramural Research Program of the Institute of Digestive and Kidney Diseases (C.D.), National Institutes of Health (C.D.), and in part by R01 DE12728 from the National Institutes of Health, USA (T.W.).

Supplementary material

Supplementary material for this article is available at
http://dev.biologists.org/cgi/content/full/132/21/4755/DC1

References

Arman, E., Haffner-Krausz, R., Gorivodsky, M. and Lonai, P. (1999). Fgfr2 is required for limb outgrowth and lung-branching morphogenesis. *Proc. Natl. Acad. Sci. USA* **96**, 11895-11899.

Boulet, A. M., Moon, A. M., Arenkiel, B. R. and Capecchi, M. R. (2004). The roles of Fgf4 and Fgf8 in limb bud initiation and outgrowth. *Dev. Biol.* **273**, 361-372.

Chen, Y., Knezevic, V., Ervin, V., Hutson, R., Ward, Y. and Mackem, S. (2004). Direct interaction with Hoxd proteins reverses Gli3-repressor function to promote digit formation downstream of Shh. *Development* **131**, 2339-2347.

Chiang, C., Litingtung, Y., Lee, E., Young, K. E., Corden, J. L., Westphal, H. and Beachy, P. A. (1996). Cyclopia and defective axial patterning in mice lacking Sonic hedgehog gene function. *Nature* **383**, 407-413.

Corson, L. B., Yamanaka, Y., Lai, K. M. and Rossant, J. (2003). Spatial and temporal patterns of ERK signaling during mouse embryogenesis. *Development* **130**, 4527-4537.

Coumoul, X. and Deng, C. X. (2003). Roles of FGF receptors in mammalian development and congenital diseases. *Birth Defects Res. C Embryo Today* **69**, 286-304.

Crossley, P. H. and Martin, G. R. (1995). The mouse Fgf8 gene encodes a family of polypeptides and is expressed in regions that direct outgrowth and patterning in the developing embryo. *Development* **121**, 439-451.

Davenport, T. G., Jerome-Majewska, L. A. and Papaioannou, V. E. (2003). Mammary gland, limb and yolk sac defects in mice lacking Tbx3, the gene mutated in human ulnar mammary syndrome. *Development* **130**, 2263-2273.

Davis, A. P. and Capecchi, M. R. (1996). A mutational analysis of the 5′ HoxD genes: dissection of genetic interactions during limb development in the mouse. *Development* **122**, 1175-1185.

Deng, C. X., Wynshaw-Boris, A., Shen, M. M., Daugherty, C., Ornitz, D. M. and Leder, P. (1994). Murine FGFR-1 is required for early postimplantation growth and axial organization. *Genes Dev.* **8**, 3045-3057.

Dudley, A. T., Ros, M. A. and Tabin, C. J. (2002). A re-examination of proximodistal patterning during vertebrate limb development. *Nature* **418**, 539-544.

Dunn, N. R., Winnier, G. E., Hargett, L. K., Schrick, J. J., Fogo, A. B. and Hogan, B. L. (1997). Haploinsufficient phenotypes in Bmp4 heterozygous null mice and modification by mutations in Gli3 and Alx4. *Dev. Biol.* **188**, 235-247.

Fallon, J. F., Lopez, A., Ros, M. A., Savage, M. P., Olwin, B. B. and Simandl, B. K. (1994). FGF-2: apical ectodermal ridge growth signal for chick limb development. *Science* **264**, 104-107.

Guha, U., Gomes, W. A., Kobayashi, T., Pestell, R. G. and Kessler, J. A. (2002). In vivo evidence that BMP signaling is necessary for apoptosis in the mouse limb. *Dev. Biol.* **249**, 108-120.

Hajihosseini, M. K., Lalioti, M. D., Arthaud, S., Burgar, H. R., Brown, J. M., Twigg, S. R., Wilkie, A. O. and Heath, J. K. (2004). Skeletal development is regulated by fibroblast growth factor receptor 1 signalling dynamics. *Development* **131**, 325-335.

Heldin, C. H., Miyazono, K. and ten Dijke, P. (1997). TGF-beta signalling from cell membrane to nucleus through SMAD proteins. *Nature* **390**, 465-471.

Hou, J. Z., Kan, M. K., McKeehan, K., McBride, G., Adams, P. and McKeehan, W. L. (1991). Fibroblast growth factor receptors from liver vary in three structural domains. *Science* **251**, 665-668.

Katagiri, T., Boorla, S., Frendo, J. L., Hogan, B. L. and Karsenty, G. (1998). Skeletal abnormalities in doubly heterozygous Bmp4 and Bmp7 mice. *Dev. Genet.* **22**, 340-348.

Kawakami, Y., Rodriguez-Leon, J., Koth, C. M., Buscher, D., Itoh, T., Raya, A., Ng, J. K., Esteban, C. R., Takahashi, S., Henrique, D. et al. (2003). MKP3 mediates the cellular response to FGF8 signalling in the vertebrate limb. *Nat. Cell Biol.* **5**, 513-519.

Laufer, E., Nelson, C. E., Johnson, R. L., Morgan, B. A. and Tabin, C. (1994). Sonic hedgehog and Fgf-4 act through a signaling cascade and feedback loop to integrate growth and patterning of the developing limb bud. *Cell* **79**, 993-1003.

Li, C., Guo, H., Xu, X., Weinberg, W. and Deng, C. X. (2001). Fibroblast growth factor receptor 2 (Fgfr2) plays an important role in eyelid and skin formation and patterning. *Dev. Dyn.* **222**, 471-483.

Lowe, L. A., Yamada, S. and Kuehn, M. R. (2000). HoxB6-Cre transgenic mice express Cre recombinase in extra-embryonic mesoderm, in lateral plate and limb mesoderm and at the midbrain/hindbrain junction. *Genesis* **26**, 118-120.

Mansour, S. L., Goddard, J. M. and Capecchi, M. R. (1993). Mice homozygous for a targeted disruption of the proto-oncogene int-2 have developmental defects in the tail and inner ear. *Development* **117**, 13-28.

Mariani, F. V. and Martin, G. R. (2003). Deciphering skeletal patterning: clues from the limb. *Nature* **423**, 319-325.

Martin, G. R. (1998). The roles of FGFs in the early development of vertebrate limbs. *Genes Dev.* **12**, 1571-1586.

Massague, J. (1998). TGF-beta signal transduction. *Annu. Rev. Biochem.* **67**, 753-791.

McLeod, M. J. (1980). Differential staining of cartilage and bone in whole mouse fetuses by alcian blue and alizarin red S. *Teratology* **22**, 299-301.

Muenke, M., Schell, U., Hehr, A., Robin, N. H., Losken, H. W., Schinzel, A., Pulleyn, L. J., Rutland, P., Reardon, W., Malcolm, S. et al. (1994). A common mutation in the fibroblast growth factor receptor 1 gene in Pfeiffer syndrome. *Nat. Genet.* **8**, 269-274.

Mukhopadhyay, M., Shtrom, S., Rodriguez-Esteban, C., Chen, L., Tsukui, T., Gomer, L., Dorward, D. W., Glinka, A., Grinberg, A., Huang, S. P. et al. (2001). Dickkopf1 is required for embryonic head induction and limb morphogenesis in the mouse. *Dev. Cell* **1**, 423-434.

Nelson, D. K. and Williams, T. (2004). Frontonasal process-specific disruption of AP-2alpha results in postnatal midfacial hypoplasia, vascular anomalies, and nasal cavity defects. *Dev. Biol.* **267**, 72-92.

Niswander, L. and Martin, G. R. (1993). FGF-4 and BMP-2 have opposite effects on limb growth. *Nature* **361**, 68-71.

Niswander, L., Jeffrey, S., Martin, G. R. and Tickle, C. (1994). A positive feedback loop coordinates growth and patterning in the vertebrate limb. *Nature* **371**, 609-612.

Orr-Urtreger, A., Givol, D., Yayon, A., Yarden, Y. and Lonai, P. (1991). Developmental expression of two murine fibroblast growth factor receptors, flg and bek. *Development* **113**, 1419-1434.

Orr-Urtreger, A., Bedford, M. T., Burakova, T., Arman, E., Zimmer, Y., Yayon, A., Givol, D. and Lonai, P. (1993). Developmental localization of the splicing alternatives of fibroblast growth factor receptor-2 (FGFR2). *Dev. Biol.* **158**, 475-486.

Partanen, J., Schwartz, L. and Rossant, J. (1998). Opposite phenotypes of hypomorphic and Y766 phosphorylation site mutations reveal a function for Fgfr1 in anteroposterior patterning of mouse embryos. *Genes Dev.* **12**, 2332-2344.

Qu, S., Li, L. and Wisdom, R. (1997). Alx-4: cDNA cloning and characterization of a novel paired-type homeodomain protein. *Gene* **203**, 217-223.

Revest, J. M., Spencer-Dene, B., Kerr, K., De Moerlooze, L., Rosewell, I. and Dickson, C. (2001). Fibroblast growth factor receptor 2-IIIb acts upstream of Shh and Fgf4 and is required for limb bud maintenance but not for the induction of Fgf8, Fgf10, Msx1, or Bmp4. *Dev. Biol.* **231**, 47-62.

Riddle, R. D., Johnson, R. L., Laufer, E. and Tabin, C. (1993). Sonic-hedgehog mediates the polarizing activity of the zpa. *Cell* **75**, 1401-1416.

Saunders, J. W., Jr (2002). Is the progress zone model a victim of progress? *Cell* **110**, 541-543.

Savage, M. P., Hart, C. E., Riley, B. B., Sasse, J., Olwin, B. B. and Fallon, J. F. (1993). Distribution of FGF-2 suggests it has a role in chick limb bud growth. *Dev. Dyn.* **198**, 159-170.

Soriano, P. (1999). Generalized lacZ expression with the ROSA26 Cre reporter strain. *Nat. Genet.* **21**, 70-71.

Summerbell, D. and Wolpert, L. (1973). Precision of development in chick limb morphogenesis. *Nature* **244**, 228-230.

Summerbell, D., Lewis, J. H. and Wolpert, L. (1973). Positional information in chick limb morphogenesis. *Nature* **244**, 492-496.

Sun, X., Lewandoski, M., Meyers, E. N., Liu, Y. H., Maxson, R. E., Jr and Martin, G. R. (2000). Conditional inactivation of Fgf4 reveals complexity of signalling during limb bud development. *Nat. Genet.* **25**, 83-86.

Sun, X., Mariani, F. V. and Martin, G. R. (2002). Functions of FGF signalling from the apical ectodermal ridge in limb development. *Nature* **418**, 501-508.

Suzuki, T., Takeuchi, J., Koshiba-Takeuchi, K. and Ogura, T. (2004). Tbx genes specify posterior digit identity through Shh and BMP signaling. *Dev. Cell* **6**, 43-53.

Tabin, C. (1995). The initiation of the limb bud: growth factors, Hox genes, and retinoids. *Cell* **80**, 671-674.

Takahashi, M., Tamura, K., Buscher, D., Masuya, H., Yonei-Tamura, S., Matsumoto, K., Naitoh-Matsuo, M., Takeuchi, J., Ogura, K., Shiroishi, T. et al. (1998). The role of Alx-4 in the establishment of anteroposterior polarity during vertebrate limb development. *Development* **125**, 4417-4425.

Tickle, C. and Munsterberg, A. (2001). Vertebrate limb development–the early stages in chick and mouse. *Curr. Opin. Genet. Dev.* **11**, 476-481.

Verheyden, J. M., Lewandoski, M., Deng, C., Harfe, B. D. and Sun, X. (2005). Conditional inactivation of *Fgfr1* in mouse defines its role in limb bud establishment, outgrowth and digit patterning. *Development* **132**, 4235-4245.

Werner, S., Duan, D. S., de Vries, C., Peters, K. G., Johnson, D. E. and Williams, L. T. (1992). Differential splicing in the extracellular region of fibroblast growth factor receptor 1 generates receptor variants with different ligand-binding specificities. *Mol. Cell. Biol.* **12**, 82-88.

Wolpert, L. (2002). Limb patterning: reports of model's death exaggerated. *Curr. Biol.* **12**, R628-R630.

Xu, X., Weinstein, M., Li, C., Naski, M., Cohen, R. I., Ornitz, D. M., Leder, P. and Deng, C. (1998). Fibroblast growth factor receptor 2 (FGFR2)-mediated reciprocal regulation loop between FGF8 and FGF10 is essential for limb induction. *Development* **125**, 753-765.

Xu, X., Weinstein, M., Li, C. and Deng, C. X. (1999). Fibroblast growth factor receptors (FGFRs) and their roles in limb development. *Cell Tissue Res.* **296**, 33-43.

Xu, X., Qiao, W., Li, C. and Deng, C. X. (2002). Generation of Fgfr1 conditional knockout mice. *Genesis* **32**, 85-86.

Yamaguchi, T. P., Harpal, K., Henkemeyer, M. and Rossant, J. (1994). fgfr-1 is required for embryonic growth and mesodermal patterning during mouse gastrulation. *Genes Dev.* **8**, 3032-3044.

Zakany, J. and Duboule, D. (1996). Synpolydactyly in mice with a targeted deficiency in the HoxD complex. *Nature* **384**, 69-71.

Zakany, J., Kmita, M. and Duboule, D. (2004). A dual role for Hox genes in limb anterior-posterior asymmetry. *Science* **304**, 1669-1672.

Zucker, R. M., Hunter, E. S., 3rd and Rogers, J. M. (1999). Apoptosis and morphology in mouse embryos by confocal laser scanning microscopy. *Methods* **18**, 473-480.